INVESTIGATION ON TEMPERATURE DISTRIBUTION AT THE TOOL-CHIP INTERFACE UNDER VARIABLE HEAT TRANSFER CONDITIONS

Wit Grzesik, Marian Bartoszuk

Summary

This papers analyzes quantitatively heat transfer problem in the cutting tool in a steady–state orthogonal cutting when using uncoated carbide tools and the X5CrNi18-9 stainless steel as a work material. Finite Difference Approach (FDA) is applied to predict the changes of temperature distribution, and both average and maximum temperatures at the tool-chip interface, resulting from different the heat flux configuration. Moreover, some realistic computing errors due to possible measuring variations of the tool-chip contact length and the intensity of heat source were considered in simulations. Basically, uniformly distributed plane, symmetrical and asymmetrical triangular, and symmetrical and asymmetrical trapezoid-type heat flux configurations were accounted for. It was found that the assumption of an asymmetrical trapezoidal shape of heat flux configuration provides the simulated results closer to the experimental data.

Keywords: orthogonal cutting, temperature distribution, FDA

Badania rozkładu temperatury w strefie kontaktu wiór-powierzchnia natarcia w warunkach zmiennego ciepła

Streszczenie

W artykule przedstawiono analizę transferu ciepła w narzędziach skrawających w przypadku skrawania ortogonalnego w warunkach procesu ustalonego, przy użyciu niepowlekanych ostrzy węglikowych i skrawaniu stali austenitycznej X5CrNi18-9. Do symulowania zmian rozpływu ciepła w strefie skrawania stosowano metodę różnic skończonych. Średnią oraz maksymalną temperaturę kontaktu wyznaczano dla różnych konfiguracji źródeł ciepła. W obliczeniach uwzględniano wpływ zmiany długości kontaktu oraz intensywność źródła ciepła. Uwzględniono podstawowe, płaskie źródło ciepła, źródło trójkątne oraz trapezowe symetryczne i niesymetryczne. Udowodniono, że trapezowy asymetryczny kształt źródła ciepła pozwala uzyskać dobre przybliżenie wyników symulacji do danych eksperymentalnych.

Słowa kluczowe: skrawanie ortogonalne, rozkład temperatury, metoda różnic skończonych

1. Introduction

For the past fifty years metal cutting researchers have developed many modelling techniques including analytical techniques, slip-line solutions,

Address: Prof. Wit GRZESIK, Ph.D, Eng., Marian BARTOSZUK, D.Sc., Eng., Dept. of Manufacturing Engineering and Production Automation, Opole University of Technology, 45-271 Opole, 5th Mikolajczyka St., grzesik@po.opole.pl

empirical approaches and simulation techniques. Although the finite element method (FEM) has particularly become the main tool for simulating metal cutting processes, the finite different approach (FDA) and boundary element method (BEM) have also occasionally been applied to study the forward thermal problems in machining [1, 2, 3, 4].

Smith and Armarego [5] first predicted temperature in orthogonal cutting with the finite difference approach (FDA), based on the classical thin shear zone model and a cylindrical polar coordinate system of mesh for the tool. Lazoglu and Altintas [6] have applied the FDA method for the predictions of steady-state tool and chip temperature fields in continuous machining and transient temperature variation in interrupted cutting (milling) of different materials such as steels and aluminum alloys. Recently, Grzesik et al. [3, 7] have developed a special variant of the finite difference method, called the method of elementary balances (MBE), in which difference equations are defined based on balances of energy produced for all discrete elements of the model. As a result, the tool temperature fields in continuous (orthogonal) machining of X5CrNi18-9 steel with uncoated and coated carbide tools were predicted. These predictions provide a detailed view of the changes in the 2D-thermal field inside the tool body as a function of cutting speed for the defined friction conditions and values of the heat partition coefficient. Special attention was paid to temperature distribution curves at the tool-chip and work-flank interfaces. Moreover, some possible sources of computed errors, as for example the number of iterations, magnitude of the heat flux, and distribution of the temperature along the contact length were accounted for. It is concluded that the assumption of a classical heat transfer model with a uniform distribution of the heat flux can be a substantial barrier in providing realistic process data [7].

In general, in the simulations of mechanical and thermal aspects of the cutting process, the problem of measuring and computing inaccuracies related to both input data or process variables is either neglected or taken into consideration fragmentarily. On the other hand, some estimations revealed [8, 9] that providing wrong data to the simulation program can result in substantial under- or overestimation of the predicted process quantities. For example, Ostafiev et al. [9] obtained quite different temperature fields when changing heat transfer conditions, especially the heat flux transfer peculiarity in the cutting tool. The other sources of discrepancies between calculated and measured values of tool temperatures can lay in the heat flux reflection from the cutting tool tip surfaces, temperature dependence of the thermal properties of tool material and workpiece temperature rise. Surprisingly, it was proven that the heat flux distribution iterated only small changes in the temperature field. In contrast, it is suggested [10] that the shape of heat source influences the location of the maximum interface temperature, but it remains the same value. Moreover, the assumption of both triangular and trapezoid-type heat distribution on the rake

face results in better agreement of analytically predicted values with those obtained numerically, using FEM, by Tay [1]. In Ref. [7] a finite difference model was developed to map the temperature distribution along the interface and inside the selected coating/substrate area and to compute the average interface temperature. The FDA simulations confirmed a distinct influence of coatings on the interface temperatures and their distributions due to visible changes in the heat partition coefficient and the contact length.

This paper provides unique isothermal maps for temperature distribution in a P20 carbide tool when machining an X5CrNi18-9 stainless steel at different cutting speeds ranging from 120 to 160 m/min. Several possible sources of errors and discrepancies between the measurements and the results of numerical computations are discussed. It was achieved by the input of given variations in the heat flux intensity and the tool-chip contact length to the FDA program for four different shapes of heat source. In order to verify the modelling results the average interface temperature was also assessed experimentally using the classical tool-workpiece thermocouple technique. It can be concluded that the FDA-based modelling of the tool-chip interface temperature distribution is a very robust computing method and allows to establish the variations of heat transfer along the interface.

2. Simulation procedure

2.1. Process conditions

Characteristic features of the process: dry, orthogonal.
Cutting tool material: uncoated ISO P20 carbide grade.
Work material: stainless steel (X5CrNi18-9).
The following machining conditions were kept in these computations:

- cutting speeds = 120, 140 and 160 m/min;
- feed rate = 0.16 mm/rev;
- depth of cut = 2 mm;
- cutting edge is ideally sharp.

2.2. Experimental data

a) Contact length obtained experimentally using computerized image processing.
b) Thermal conductivity (λ_W) and corresponding thermal diffusivity (α_W) as function as temperature (t):

$$\lambda_W = 5{,}744\text{E} - 006t^2 + 0{,}018t + 33{,}339 \tag{1}$$

$$\alpha_W = \lambda / c_p \rho \tag{2}$$

where: c_p is the specific heat and ρ is the density of sintered carbide grade used.

Calculated values of λ_W are equal to 47.11, 47.25 and 47.43 W/(mK) for the selected cutting speeds. Corresponding values of α_W are equal to 2.75×10^{-5}, 2.77×10^{-5} and 2.79×10^{-5} m^2/s.

c) Calculation of the heat amount (cutting energy) generated at the tool-chip interface:

$$Q_c = F_\gamma v_{ch} \tag{3}$$

where: F_γ is friction force, v_{ch} is chip velocity.

d) Calculation of the heat partition coefficient based on the algorithm proposed by Reznikov (R_{ch}) [7]:

$$R_{ch} = 1/\left(1 + 1.5\lambda_T / \lambda_W \sqrt{\alpha_W / \alpha_T}\right) \tag{4}$$

where: λ, α – the thermal conductivity and diffusivity for work (W) and tool (T) materials, respectively.

e) Four different shapes of heat source (Fig.1) were selected, keeping the same area of three geometrical figures, i.e. rectangle, triangle and trapezoid.

2.3. Simulation algorithm

In this study a special variant of the FDM, called the method of elementary balances (MBE), in which difference equations are defined based on balances of energy for all discrete elements of the model was applied [3]. This method uses only the Fourier's law and typical calculation mesh available in Microsoft Excel program. In particular, each cell within the calculation sheet is assigned to one discrete element of the analytical model considered. As a result, the model is built as a set of cells including adequate formulae and values, which finally represents both geometrical and physical features of the modeled process. Formulae are introduced according to the explicit method of the difference procedure. Moreover, the process conditions for zero intrinsic heat source $\dot{q}_v = 0$ and a steady two-dimensional heat flow problem were assumed.

Therefore, the partial differential equation for the heat conduction rates in two orthogonal directions x and y, expressed by Fourier's heat conduction law, can be transformed to the following finite difference form [3]:

$$\frac{T_{i-1,j} - 2T_{i,j} + T_{i+1,j}}{(\Delta x)^2} + \frac{T_{i,j-1} - 2T_{i,j} + T_{i,j+1}}{(\Delta y)^2} = 0 \tag{5}$$

The difference equation (5) can be solved numerically using eight specific, linear and corner, boundary conditions described in [3]. On average, FDA-based temperature simulations involve (2-2.5) × 10^4 iterations.

3. Simulation Results

3.1. Temperature fields inside the tool

The influence of the heat source shape on the distribution of isotherms within the monolithic carbide tool is illustrated in Figures 2-4.

Heat source shape	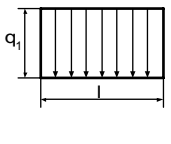 Version I	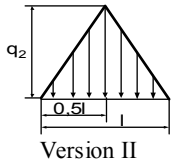 Version II	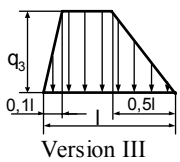 Version III	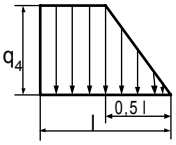 Version IV
Max. value of q	q_1	$q_2 = 2q_1$	$q_3 = 1{,}43q_1$	$q_4 = 1{,}33q_1$

Fig. 1. Shapes of heat source used in the FD simulations

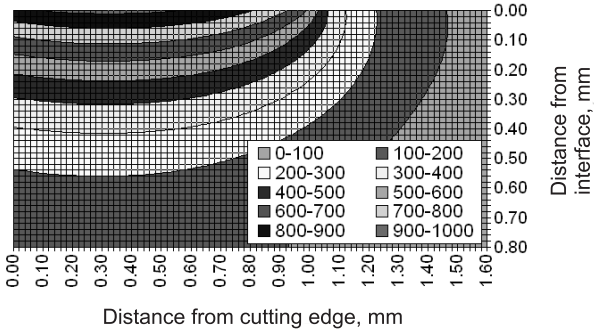

Fig. 2. Temperature field in the tool for uniformly distributed heat source and cutting speed v_c = 160 m/min

As shown in Fig. 2, the maximum temperature is localized approximately in half the contact length and coincides well with classical literature arrangement

[11]. For this case, the average and maximum temperatures computed for the cutting speed of 160 m/min are equal to 860°C and 920°C, respectively.

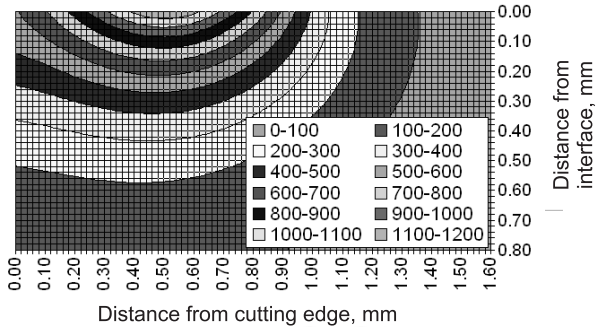

Fig. 3. Temperature field in the tool for triangular heat source and cutting speed v_c = 160 m/min

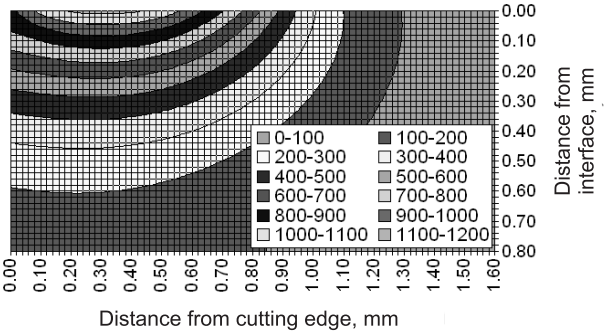

Fig. 4. Temperature field in the tool for Trapezoidal heat source (case III) and cutting speed v_c = 160 m/min

As can be observed in Figures 3 and 4, the assumption of triangular and trapezoidal heat source distribution causes the isotherm shapes and maximum temperatures to be different from those for uniform heat source from Fig. 2. Whereas, for all three cases considered, for which the average temperatures are practically the same, the maximum values for triangular and trapezoidal (case III) heat sources increase up to 1190°C and 1130°C, respectively.

3.2. Temperature at the rake face

The distribution of tool-chip interface temperature determined for all models of heat source, along with the measured average temperature, are

integrally presented in Fig. 5. It is evident from Fig. 5 that the shape of heat source influences both the peak temperature and its location at the interface. Particularly, triangular heat source can develop peak temperature of 170°C, higher than for commonly used plane heat distribution. At lower cutting speeds the predicted peak temperatures were even 200-225°C higher. The differences in computed and measured temperatures are compared for the cutting speed of 160 m/min, in Fig. 6.

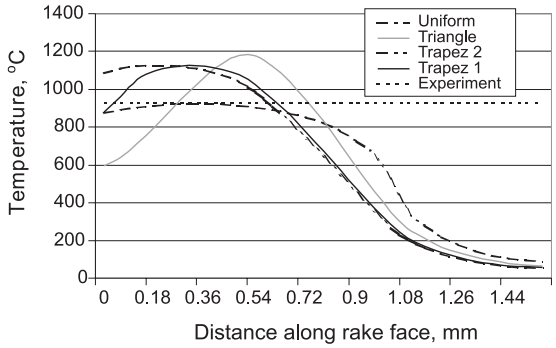

Fig. 5. Distribution of temperature at the tool-chip interface for different heat source shapes and cutting speed v_c = 160 m/min

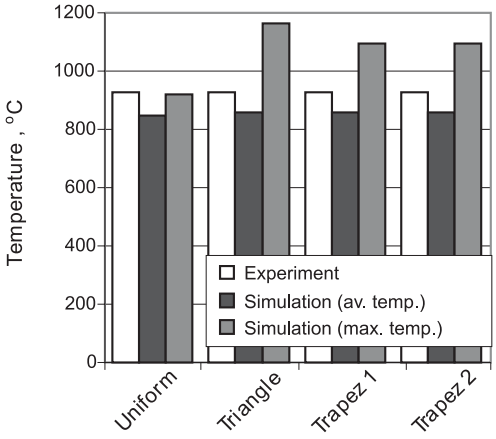

Fig. 6. Comparison of predicted temperature from Fig. 5 with measured values for cutting speed v_c = 160 m/min

3.3. Temperature changes at variable heat transfer conditions

As mentioned in Section 1, the estimation of interface temperatures was extended over the consideration of two basic variables, including the heat source intensity (its width) and its length. This approach results directly from possible distinct measuring inaccuracies of friction force and contact length. Based on long-time experiments in this metal cutting aspects, three levels of variations were assumed, i.e. ±5%, ±10% and ±15%.

In the simulation with variable heat source intensity, the reference values of the heat flux are set at 67.85, 76.62 and 99.10 MW/m^2 for cutting speed of 120, 140 and 160 m/min, respectively. Appropriate simulations results are shown in Figures 7-10. As shown in Fig. 7 and 8 the simulation results in underestimating the average temperatures in relation to the measurements.

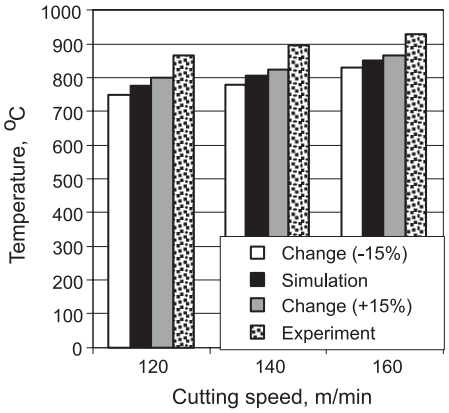

Fig. 7. Influence of changes of tool-chip contact length on the average temperature for uniform heat source and variable cutting speed

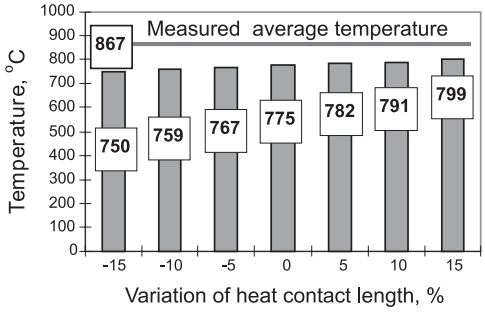

Fig. 8. Changes of average interface temperature due to variations in the contact length (uniform heat source and cutting speed v_c = 120 m/min)

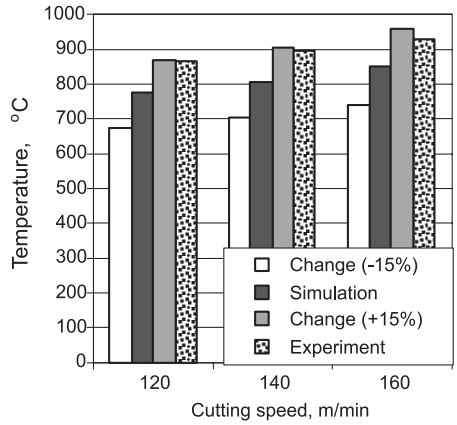

Fig. 9. Influence of changes of heat source intensity on the average temperature for uniform heat source and variable cutting speed

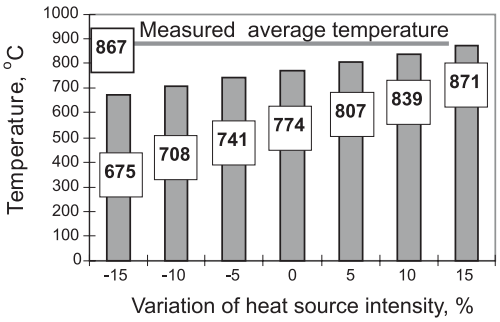

Fig. 10. Changes of average interface temperature due to variations in heat source intensity (uniform heat source and v_c=120 m/min)

In this case, satisfactory agreement was achieved for enlarged contact length by 15%. When considering only simulation results (Fig. 8), this effect is not so pronounced and is in the range ±4%. On the other hand, the same variations of heat flux (Figs. 9 and 10) generate visible changes in the average interface temperature. As documented in Fig. 9, the increase of the experimentally determined heat flux by 15% shifted the esteemed values of temperature closer to the recorded values. It can be seen in Fig. 9 that this effect was obtained for all three cutting speeds considered.

It may be concluded, based on Figures 8 and 10, that the basic source of the discrepancy between FDA simulations and thermocouple-based measurements lays in an important underestimation of the heat flux.

4. Conclusions

1. The simulation accuracy depends not only on the model formulation, including both initiating and boundary conditions, but primarily on the shape of heat source.
2. Acceptable agreement between computed and measured values of the average interface temperatures was obtained for trapezoidal shape of the heat source, similar to the distribution of contact shear stresses.
3. It was found that the contact length is a secondary important factor in the estimation of proper values of the average interface temperature.
4. One of the main findings is that the discrepancy between simulations and measurements can result from underestimation of the heat flux.

References

[1] A.A.O. TAY: Review of methods of calculating machining temperature. *J. Mat. Proc. Technol*., **36**(1993), 225-257.
[2] F. KLOCKE, T. BECK, S. HOPPE, T. KRIEG et al.: Examples of FEM application in manufacturing technology. *J. Mat. Proc. Technology*, **120**(2002), 450-457.
[3] W. GRZESIK, M. BARTOSZUK, P. NIESLONY: Finite difference analysis of the thermal behaviour of coated tools in orthogonal cutting of steels. *J. Mach. Tools Manuf*., **44**(2004), 1451-1462.
[4] Ch.L. CHAN, A. CHANDRA: A boundary element method analysis of the thermal aspects of metal cutting process. *J. Eng. Ind*., **113**(1991), 311-319.
[5] A.J.R. SMITH, E.J.A. ARMAREGO: Temperature prediction in orthogonal cutting with a finite difference approach, *Annals of the CIRP*, **30**(1981), 9-13.
[6] I. LAZOGLU, Y. ALTINTAS: Prediction of tool and chip temperature in continuous and interrupted machining. *J. Mach. Tools Manufact*., **42**(2002), 1011-1022.
[7] W. GRZESIK: Analytical models based on composite layer for computation of tool-chip interface temperatures in machining steels with multilayer coated cutting tools, *Annals of the CIRP*, **54**(2005)1, 91-94.
[8] W. GRZESIK: Simulation of computational errors for tool-chip interface temperatures resulting from geometrical and thermal features of the heat source, presentation on WG(C) on thermal measurement in manufacturing, Paris 2004.
[9] V. OSTAFIEV, A. KHARKEVICH, K. WEINERT, S. OSTAFIEV: Tool heat transfer in orthogonal metal cutting. *J. Manuf. Sci. Eng*., **121**(1999), 541-549.
[10] H.T. YOUNG, T.L. CHOU: Modelling of tool-chip interface temperature distribution in metal cutting, *J. Mech. Sci*., **36**(1994)10, 931-943.
[11] E. M. TRENT, P.K. WRIGHT: Metal cutting. Butterworth Heinemann, Boston 2000.

Received in May 2008